# Molecular dynamic study for ultrathin $Ni_3Fe$ alloy

M. D. Starostenkov  M. M. Aish
mohamedeash2@yahoo.com

**Abstract**

Molecular Dynamics (MD) simulations have been carried out on ultrathin $Ni_3Fe$ alloy with face-centered cubic (FCC) lattice upon application of uniaxial tension at nanolevel with a speed of 20 m/s. the deformation corresponds to the direction <001>. To the calculated block of crystal - free boundary conditions were applied in the directions <100>, <010>. Morse potential was employed to carry out three dimensional molecular dynamics simulations. A computer experiment was performed at a temperature corresponding to 300 K and 1000 K. MD simulation used to investigate the effect of long of ultrathin $Ni_3Fe$ alloy on the nature of deformation and fracture. The engineering stress–time diagrams obtained by the MD simulations of the tensile specimens of these ultrathin $Ni_3Fe$ alloy show a rapid increase in stress up to a maximum followed by a gradual drop to zero when the specimen fails by ductile fracture. The feature of deformation energy can be divided into four regions: quasi-elastic, plastic, flow and failure. The yield strength decreased with increasing long of alloy. The results showed that breaking position depended on the alloy length.

## 1 Introduction

A three-dimensional alloy with rectangular cross-section cut from single-crystal bulk was simulated as in fig (1). The initial atomic configuration was positioned at the ideal lattice sites. The X, Y, and Z coordinate axes represent the lattice directions [100], [001], and [010], respectively. The estimated size of the crystal unit was for various experiments of 252 atoms (6 atoms along the edges at the bottom and 6 - in height) to 1764 atoms (90 atoms along the edges at the bottom and 6 - in height). The total sample consists of two parts. One part was designed as the active zone in which atoms move according to the inter-atomic potential; the other part was the boundary zone where positions of atoms were given by prescribed boundary conditions. The periodic boundary condition was applied in the length direction, i.e., the Z axis. The surfaces in the X and Y directions were free. The existence of those free surfaces will result in relaxation motion of the atoms near the surfaces, which then minimizes the total energy of the system.

In each simulation the temperature was kept constant by the direct velocity scaling method [1, 2]. After full relaxation, extension strain loading was applied by uniformly scaling the Z coordinates. The atoms at each end were constrained, and can only displace in the Z direction during each loading step. The stepwise tensile strain was 0.02. It was relaxed for some time in each step. Both the strain step and relaxation time determine the strain rate. The tension/relaxation step was repeated until the model fails.

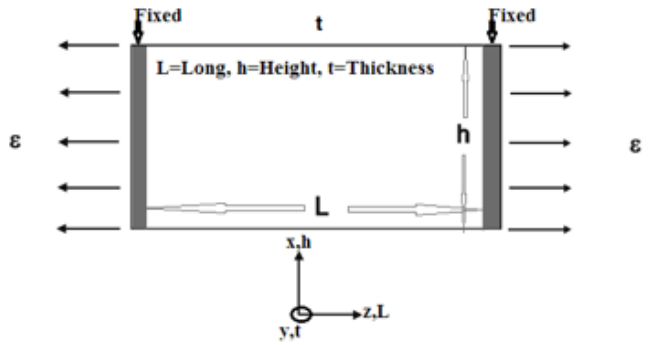


Figure 1: Geometry of alloy subjected to uniaxial tension under constant strain rate.

## 2 Model and simulation method

In this paper for calculating the dynamics of the atomic structure of the method of molecular dynamics using paired Morse potential function [2-5], suitable in terms of their computing time and quality of results.

Morse pair potential was written as:

$$\varphi_{KL}(r) = D_{KL}\beta_{KL}e^{-\alpha_{KL}r}\left[\beta_{KL}e^{-\alpha_{KL}r} - 2\right], \tag{1}$$

where $\alpha_{KL}$, $\beta_{KL}$, $D_{KL}$ are parameters defining the interaction of pairs of atoms of type $K$ and $L$; $r$ is the distance between the atoms. The specific potential parameters were listed in [2, 6] when tie potential was determined, the atomic force $F$ was given as the derivative of the potential energy, namely

$$F = \frac{d\varphi_{KL}(r)}{dr}. \tag{2}$$

The object of investigation was taken ultrathin systems of $Ni_3Fe$ alloy structure was presented in the form of a face-centered cubic cell. A computer experiment was performed at a temperature corresponding to 300 K and 1000 K, at any stage of deformation involving the possibility of chilling calculation unit for detailed analysis of the structural changes occurring in it [7-9].

## 3 Atom snapshot during tensile deformation

To visualize the tensile deformation process of the $Ni_3Fe$ alloy at 300 K and 1000 K, snapshots of atomic rearrangements were shown in Fig (2, 3) after relaxation, the surface atoms move a little and the whole configuration maintains regularity when there was no strain load, as displayed in Fig.2a, 3a. When the model stretches in the height direction, necking appears near the middle of the model and then becomes increasingly distinct, and the deformation concentrates in the neck region as shown in Fig.2d and e. In the end, the plastic deformation causes ductile shear fracture as shown in Fig.2e. This deformation evolution was also different from that of $Ni_3Fe$ alloy, in which there was no necking and brittle fracture occurs suddenly near the middle of the model. [6] From Fig.2 and 3 the tensile mechanism of the atomistic simulations at the nanometer dimension shows results that agree with the mechanism of plasticity observed in macroscale experiments.

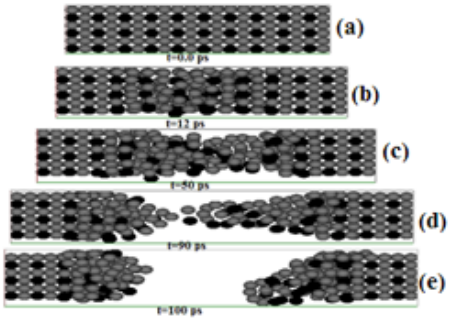


Figure 2: Snapshots of the atomic configuration rearrangement of a 6x6x12 $Ni_3Fe$ alloy at a temperature of 300 K and. The configurations presented correspond to the following times: (a) 0 ps, (b) 12 ps, (c) 50 ps, (d) 90 ps and (e) 100 ps.

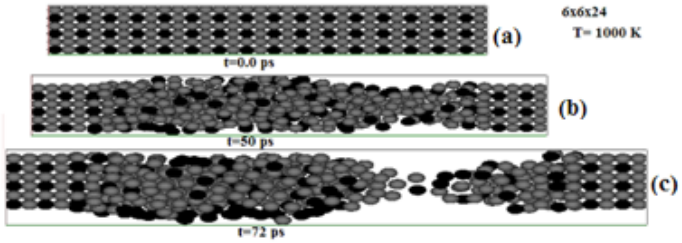


Figure 3: Snapshots of the atomic configuration rearrangement of a 6x6x24 $Ni_3Fe$ alloy at a temperature of 1000 K and. The configurations presented correspond to the following times: (a) 0 ps, (b) 50 ps and (c) 72 ps.

## 4 Stages of deformation

The experiments were obtained plots of the stored energy of deformation of the time, reflecting the processes in the nanowire during deformation. There were four stages of deformation: the quasi-elastic deformation (I), plastic deformation (II), the breaking (flow) (III), and failure (IV). At all lengths, in the first stage there was almost linear increase in stress. The initial stage quasi-elastic area there was only relative displacement of atoms and there were no defects. Therefore, in this region the energy stored varies periodically. This stage was completed in 15 ps for 6x6x6 $Ni_3Fe$ alloy and 110 ps for 6x6x90. The sharp fall takes place only at the point of transition from the first to second stages of deformation (Fig. 4 a). Experiments have shown that when the volume increases the first stage of deformation was widened, and also the second stage was narrowed. In fig 4.c the plastic deformation disappears.

## 5 Effect of alloy length and mechanical properties

To discuss the effect of nanowire length, a constant base of 6x6 nm was set and the length was varied in the range 5–90 nm in the simulations. In this work, MD simulations were performed for ultrathin Ni nanowire subject to uniaxial tensile strain loading. Fig.5 shows the simulated ultimate strength of ultrathin $Ni_3Fe$ nanowires as a function of nanowire length for different temperatures. As expected, the nanowire strength decreases with increase of temperature for all the given nanowire length. It was believed that the temperature softening results from the weaker bonds between atoms caused by the increasing temperature. By comparing the results in Fig.5, it was found that for all the temperatures and nanowire

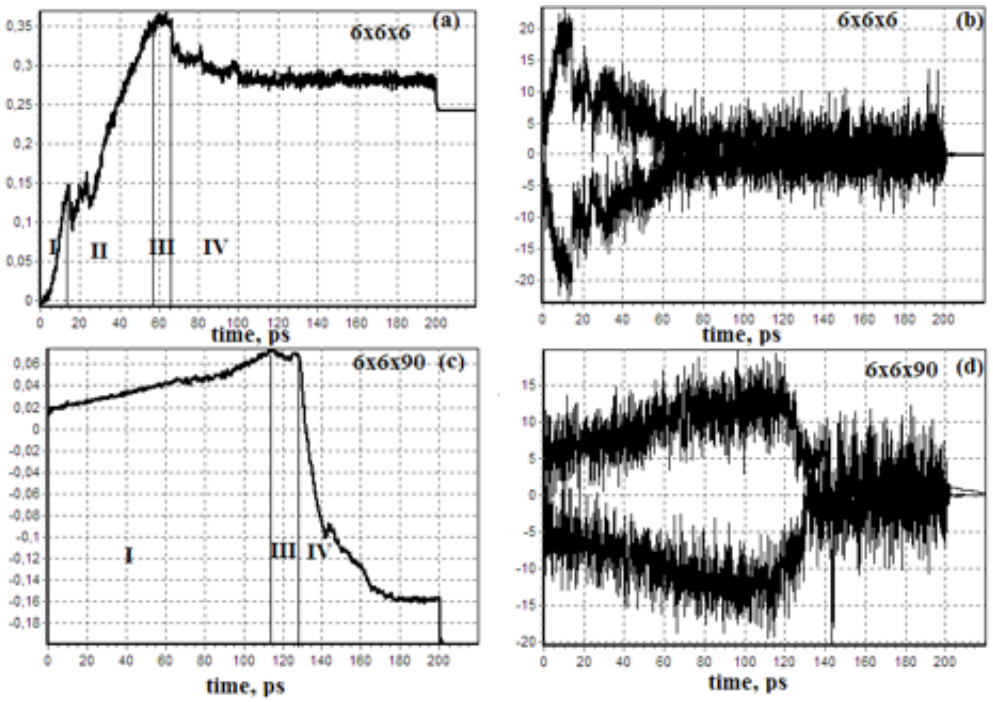


Figure 4: The dependence of the stored energy of deformation of the experiment at 300K for Ni3Fe alloy 6 x 6 x 6 (a), the relation of stress with time at temperatures 300K for $Ni_3Fe$ alloy -6 x 6 x 6 (b), the dependence of the stored energy of deformation of the experiment at 300K for $Ni_3Fe$ alloy 6 x 6 x 90 (c) and the relation of stress with time at temperatures 300K for Ni3Fe alloy -6 x 6 x 90 (d).

lengths', the strength becomes lower as nanowire length increases. Fig.5 shows decreases in strength with increasing nanowire length at different temperatures.

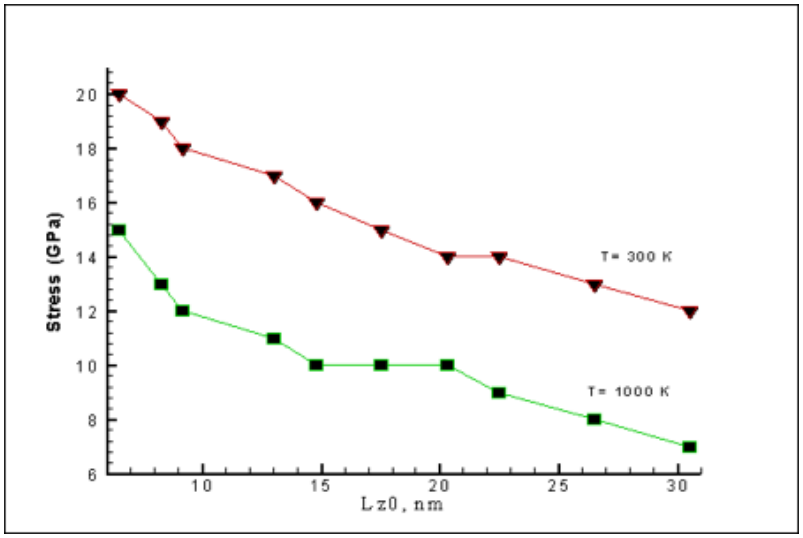


Figure 5: The simulated ultimate strength of ultrathin $Ni_3Fe$ nanowire as a function of nanowire length at 300 K and 1000 K.

## 6 Breaking

The results showed that the breaking position depended on the alloy length (table 1and 2). When it was less than 21.5nm, the most probable breaking position was located at the center of the alloys. However, it gradually shifted to the ends as the alloy length increased over 21.5nm as in table 1 and 2. Fig .6 presents the calculated breaking length for ultrathin $Ni_3Fe$ alloy as a function of alloy length for different temperatures. This result implies that the temperature and nanowire length may have a strong effect on the breaking position. It was worth noting, as shown in Figs.6 and 7, that the long dependence of the Breaking position was completely difference from that of the strength.

Table 19: The typical MD results of different system of ultrathin $Ni_3Fe$ alloy at 300 K including the time required to attain atomic break, the number of atoms, initial length, breaking length, yielding time, yielding stress and yielding strain and the calculated final breaking position.

| | System | N | | $l_0$ | Yielding point | | | | Breakdown | | |
|---|---|---|---|---|---|---|---|---|---|---|---|
| | | | | | σ(Gpa) | t,ps | $l_{z1.nm}$ | ε | $t$ | $l_b$ | Position |
| | | Ni | Fe | | | | | | | | |
| 1 | *6x6x6* | 189 | 63 | 20 | 15 | 7.2 | 0.107 | 60 | 9.5 | 6 | 0.107 |
| 2 | *6x6x10* | 243 | 81 | 19 | 18 | 9.3 | 0.12 | 70 | 12 | 5 | 0.12 |
| 3 | *6x6x12* | 270 | 90 | 18 | 15 | 10.2 | 0.108 | 90 | 13.8 | 7 | 0.108 |
| 4 | *6x6x20* | 378 | 126 | 17 | 30 | 14.5 | 0.115 | 126 | 19.5 | 9 | 0.115 |
| 5 | *6x6x24* | 432 | 144 | 16 | 35 | 16.4 | 0.108 | 96 | 20 | 8 | 0.108 |
| 6 | *6x6x30* | 513 | 171 | 15 | 35 | 19.5 | 0.114 | 86 | 21.5 | 9 | 0.114 |
| 7 | *6x6x36* | 594 | 198 | 14 | 65 | 24 | 0.182 | 105 | 25.8 | 9 | 0.182 |
| 8 | *6x6x40* | 648 | 216 | 14 | 60 | 25.5 | 0.133 | 70 | 25.5 | 8 | 0.133 |
| 9 | *6x6x50* | 783 | 261 | 13 | 70 | 32 | 0.207 | 116 | 33 | 11 | 0.207 |
| 10 | *6x6x90* | 1323 | 441 | 12 | 115 | 48 | 0.573 | 129 | 61 | 11 | 0.573 |

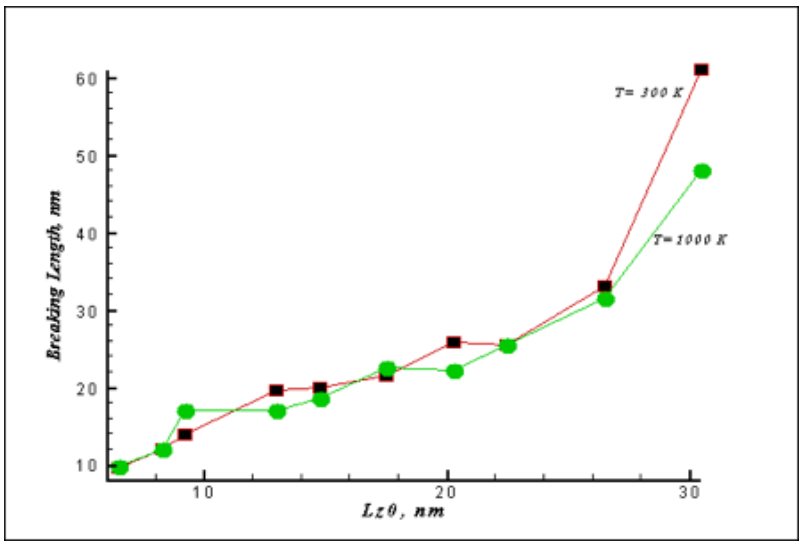


Figure 6: The calculated breaking position for ultrathin $Ni_3Fe$ alloy as a function of alloy length at 300 K and 1000 K.

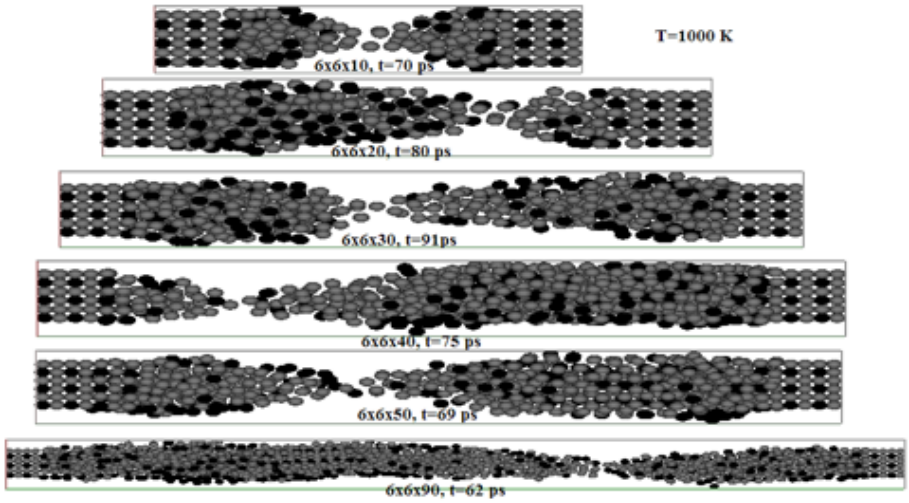


Figure 7: Necking and breaking of ultrathin $Ni_3Fe$ alloy at 1000 K under extension loading at different long.

Table 20: The typical MD results of different system of ultrathin $Ni_3Fe$ alloy at 1000 K including the time required to attain atomic break, the number of atoms, initial length, breaking length, yielding time, yielding stress and yielding strain and the calculated final breaking position.

| | System | N | | $l_0$ | Breakdown | | | Yielding point | | | |
|---|---|---|---|---|---|---|---|---|---|---|---|
| | | | | | σ(Gpa) | t,ps | $l_{z1.nm}$ | ε | t,ps | $l_b$ | Position |
| | | Ni | Fe | | | | | | | | |
| 1 | *6x6x6* | 189 | 63 | 6.5 | 15 | 10 | 7 | 0.076 | 60 | 9.8 | 4.5 |
| 2 | *6x6x10* | 243 | 81 | 8.3 | 13 | 10 | 9 | 0.084 | 70 | 12 | 6 |
| 3 | *6x6x12* | 270 | 90 | 9.2 | 12 | 15 | 10 | 0.086 | 91 | 17 | 7 |
| 4 | *6x6x20* | 378 | 126 | 13 | 11 | 30 | 14.5 | 0.115 | 80 | 17 | 10.5 |
| 5 | *6x6x24* | 432 | 144 | 14.8 | 10 | 35 | 16.5 | 0.1148 | 72 | 18.6 | 12 |
| 6 | *6x6x30* | 513 | 171 | 17.5 | 10 | 36 | 19.5 | 0.1442 | 91 | 22.5 | 9.5 |
| 7 | *6x6x36* | 594 | 198 | 20.3 | 10 | 37 | 22.5 | 0.108 | 75 | 22.2 | 6 |
| 8 | *6x6x40* | 648 | 216 | 22.5 | 9 | 40 | 24 | 0.066 | 69 | 25.5 | 10 |
| 9 | *6x6x50* | 783 | 261 | 26.5 | 8 | 45 | 29.5 | 0.113 | 59 | 31.5 | 20 |
| 10 | *6x6x90* | 1323 | 441 | 30.5 | 7 | 48 | 45 | 0.445 | 62 | 48 | 16 |

## 7 Conclusion

In this work, MD simulation has been employed to investigate the high speed tension process of ultrathin Ni3Fe nano-alloy at nano-scale. The present study demonstrates the success of modeling in reproducing the essential mechanisms of plasticity and damage on the atomic scale. Based on the above research, the following conclusions can be drawn:
1. The employment of a Morse potential was seen to be able to render an elastic, plastic and fracture behavior for the model under consideration.
2. The breaking position exhibits a distribution and the most probable breaking position presents a gradual shift from the center to the ends as the alloy length increases.
3. The stress–time curves of tensile deformation of $Ni_3Fe$ nano-alloy decrease because the first transition from elastic to plastic deformation and the first slip take place. The plastic deformation causes ductile shear fracture.

4. The tensile strength decreases with increasing length.

## References

[1] H. Rafii-Tabar, Modelling the nano-scale phenomena in condensed matter physics via computer-based numerical simulations, Phys. Rep.325, 239 (2000).

[2] Kozlov E.V., Popov L.E., Starostenkov M.D., Calculation of the Morse potential for solid gold, Russian Physics Journal. 1972. V 15. N 3. p. 395.

[3] L.A. Girifalco, V.G. Weizer, Application of the Morse Potential Function to Cubic Metals, Physical Review 114 (1959) 687.

[4] Dmitriev S.V., Ovcharov A.A., Starostenkov M.D., Kozlov Г‰.V., Physics of the Solid State. 1996. V 38. N 6. p. 996-999.

[5] M. Starostenkov , A. Yashin, N. Sinica, Structural Transformation in Nanowires CuAu I with Superstructure of L10 of Tetragonal Symmetry at Uni-Axial Tension Deformation, Key Engineering Materials (Volumes 592 - 593) pp 51-54.

[6] . X. Yang, L. Liu, P. Zhai, Q. Zhang // Computational Materials Science 44 (2009) 1390.

[7] Potekaev A.I., Dudnik E.A., Popova L.A., Starostenkov M.D. Russian Physics Journal. 2008. V 51. N 10. p. 1053-1063.

[8] M.D. Starostenkov, B.F. Demyanov, S.L. Kustov, E.G. Sverdlova, E.L. Grakhov // Computational Materials Science 14 (1999) 146.

[9] M.M. Aish , M.D. Starostenkov, Effect of volume on the mechanical properties of nickel nanowire, Mater.Phys.Mech.(MPM)No 1, Vol. 18, 2013, pages 53-62.

*M. D. Starostenkov, M.M. Aish, I. I. Polzunov Altai State Technical University, Barnaul, Russia, M.M. Aish Physics department, Faculty of science, Menoufia university, Egypt*